



## Potential *in vitro* effects of carbon nanotubes on human aortic endothelial cells

Valerie G. Walker<sup>a</sup>, Zheng Li<sup>a,1</sup>, Tracy Hulderman<sup>a</sup>, Diane Schwegler-Berry<sup>b</sup>,  
Michael L. Kashon<sup>c</sup>, Petia P. Simeonova<sup>a,\*</sup>

<sup>a</sup> Toxicology and Molecular Biology Branch, Health Effects Laboratory Division, National Institute for Occupational Safety and Health, Morgantown, WV, USA

<sup>b</sup> Pathology and Physiology Research Branch, Health Effects Laboratory Division, National Institute for Occupational Safety and Health, Morgantown, WV, USA

<sup>c</sup> Biostatistics and Epidemiology Branch, Health Effects Laboratory Division, National Institute for Occupational Safety and Health, Morgantown, WV, USA

### ARTICLE INFO

#### Article history:

Received 5 February 2009

Accepted 14 February 2009

Available online 5 March 2009

#### Keywords:

Actin  
Tubule formation  
Cytotoxicity  
SWCNT  
MWCNT

### ABSTRACT

Respiratory exposure of mice to carbon nanotubes induces pulmonary toxicity and adverse cardiovascular effects associated with atherosclerosis. We hypothesize that the direct contact of carbon nanotubes with endothelial cells will result in dose-dependent effects related to altered cell function and cytotoxicity which may play a role in potential adverse pulmonary and cardiovascular outcomes. To test this hypothesis, we examined the effects of purified single- and multi-walled carbon nanotubes (SWCNT and MWCNT) on human aortic endothelial cells by evaluating actin filament integrity and VE-cadherin distribution by fluorescence microscopy, membrane permeability by measuring the lactate dehydrogenase (LDH) release, proliferation/viability by WST-1 assay, and overall functionality by tubule formation assay. Marked actin filament and VE-cadherin disruption, cytotoxicity, and reduced tubule formation occurred consistently at 24 h post-exposure to the highest concentrations [50–150  $\mu\text{g}/10^6$  cells (1.5–4.5  $\mu\text{g}/\text{ml}$ )] for both SWCNT and MWCNT tested in our studies. These effects were not observed with carbon black exposure and carbon nanotube exposure in lower concentrations [1–10  $\mu\text{g}/10^6$  cells (0.04–0.4  $\mu\text{g}/\text{ml}$ )] or in any tested concentrations at 3 h post-exposure. Overall, the results indicate that SWCNT and MWCNT exposure induce direct effects on endothelial cells in a dose-dependent manner.

Published by Elsevier Inc.

### Introduction

Engineered carbon nanomaterials, including carbon nanotubes, have elicited a significant interest due to their unique electronic and mechanical properties. However, the small size, large surface area, and high reactivity of these materials are the main factors for potential toxicity (Donaldson et al., 2006). Carbon nanotubes (CNT), including the single- and multi-walled (SWCNT and MWCNT), will have wide-spread applications in many technological fields, thus worker/consumer exposure is likely to occur, posing emerging health concerns (Donaldson et al., 2006; Maynard et al., 2006). Initial toxicological animal studies demonstrated that pulmonary deposition of SWCNT or MWCNT causes acute pulmonary inflammation as well as chronic responses such as fibrosis (Lam et al., 2004; Warheit et al., 2004; Muller et al., 2005; Shvedova et al., 2005; Mangum et al., 2006; Li et al., 2007a; Mercer et al., 2008). Furthermore, we demonstrated that CNT respiratory exposure is associated with

adverse cardiovascular outcomes. Pulmonary deposition of SWCNT or MWCNT results in a rapid release of inflammatory mediators, activated blood cells, and thrombogenic proteins into the systemic circulation which may induce endothelial dysfunction (Erdely et al., 2009). Chronic SWCNT respiratory exposure triggers mitochondrial aortic alterations which may be associated with SWCNT-induced accelerated atherogenesis in apoE<sup>−/−</sup> mice, a model for human atherosclerosis (Li et al., 2007b). The CNT-related cardiovascular findings, are consistent with the current knowledge of the link between particulate matter in air pollution and the risk from cardiovascular diseases related to atherosclerosis (Brook et al., 2004).

The cardiovascular system may be affected through two main mechanisms including indirect effects, mediated by particle-induced pulmonary inflammation and dysfunction, or direct effects of particles that have traveled into the systemic circulation (Mills et al., 2007). It has been shown in animal models that some inhaled particles were located in tissues beyond the lung (Kreyling et al., 2002; Nemmar et al., 2002; Oberdorster et al., 2002). The proximity between epithelial type I and endothelial cell caveolar membrane structures might play a role in the particle translocation mechanisms (Heckel et al., 2004). The major unresolved question is whether particles translocate in sufficient numbers to exert a significant direct influence on vascular endothelial function (Mills et al., 2008a). Under both possible mechanisms of CNT-induced cardiovascular toxicity, endothelial

\* Corresponding author. Fax: +1 304 285 5708.

E-mail address: [psimeonova@cdc.gov](mailto:psimeonova@cdc.gov) (P.P. Simeonova).

<sup>1</sup> Current affiliation: National Center for Environmental Assessment, U.S. Environmental Protection Agency, Washington, DC, USA.

<sup>1</sup> Current affiliation: National Center for Environmental Assessment, U.S. Environmental Protection Agency, Washington, DC, USA.

cells are a potential target. Although many *in vitro* studies on CNT toxicity have been conducted (Shvedova et al., 2003; Manna et al., 2005; Monteiro-Riviere et al., 2005; Raja et al., 2007; Pacurari et al., 2008a, 2008b), the potential effects of CNT exposure on endothelial cells have not been investigated. The purpose of our studies was to evaluate potential direct toxicity of CNT on human endothelial cells, with special emphasis on the evaluation of dose-dependent effects. The dose response was select based on the hypothesis that endothelial cells are exposed to high particle concentrations at the penetration site and to low concentrations in the systemic vasculature as a result of translocation from the entrance site.

## Materials and methods

**Reagents.** Catalytically grown and purified SWCNT and MWCNT (Mitsui & Co., Ltd.) (Oberlin et al., 1976) were kindly provided by Dr. M. Endo (Shinshu University, Wakasato, Japan). Characteristics of the SWCNT (a specific surface area (BET) average 641 m<sup>2</sup>/g) and MWCNT (BET average 56 m<sup>2</sup>/g) have been described in greater detail (Kim et al., 2005; Koyama et al., 2006). Trace metal analysis by inductively coupled plasma optical emission spectrometry indicated iron content of SWCNT at 8.8% by weight and 0.27% for MWCNT. Carbon black (CB) (Elftex 12) (BET average 43 m<sup>2</sup>/g) was obtained from Cabot (Edison, NJ). Particle size according to the manufacturer for CB was 37 nm in diameter. Human aortic endothelial cells (HAEC), endothelial cell basal media (EBM-2), endothelial growth media (EGM-2) supplement bullet kit, trypsin-EDTA, trypsin neutralizing solution and HEPES buffering solution were purchased from Lonza (Walkersville, MD). The following reagents or kits were used in the current studies: rhodamine (TRITC)-phalloidin (Sigma, St. Louis, MO), WST-1 assay (Millipore, Billerica, MA), lactate dehydrogenase (LDH) assay (Biovision, Mountain View, CA), phorbol-12-myristate-13-acetate (PMA) (Calbiochem, EMD-Gibbstown, NJ), interleukin-8 (IL-8) ELISA (R&D systems, Minneapolis, MN), polyclonal VE-cadherin antibody (Axxora, San Diego, CA), BioCoat™ Angiogenesis System (BD Biosciences, Bedford, MA), and goat anti-rabbit IgG Alexa Fluor 488 antibody (Invitrogen/Molecular Probes, Carlsbad, CA).

**Cell culture.** HAEC were grown according to the manufacturer's instruction. Briefly, the cells were cultured in EBM-2 media supplemented with the EGM-2 bullet kit and grown at 37 °C with 5% CO<sub>2</sub>. All experiments were performed using cells in passages 3–6.

**Particle preparation.** SWCNT, MWCNT, and CB were diluted to a concentration of 1 mg/ml stock solution in 1× phosphate-buffered solution (PBS). The particles were vortexed for 1 min and then indirectly sonicated (Hielscher Ultrasonic) for 5 min at 4 °C immediately prior to preparing treatment-dilutions into serum-free and growth factor-free EBM-2. The dilutions were again vortexed prior to being added to the cells to insure adequate dispersion. The stock particle suspensions, prepared in the same way as for the cell exposure, were characterized by transmission electron microscopy (TEM) (Fig. 1). Both the MWCNT and SWCNT appeared with minimal aggregation in well dispersed bundles. Naturally, the CNT and nanoparticles in general, have a tendency to agglomerate. However, it is known that aggregates do not behave like a geometric particle of equal size because the greater surface area of the individual particles is mostly retained in the aggregate and may contribute to the toxicity (reviewed in Borm et al., 2006). In all experiments, the cells were treated with particles in the following concentrations: 1, 10, 50, and 150 µg/10<sup>6</sup> cells (0.04, 0.4, 1.5, and 4.5 µg/ml, respectively).

**WST-1 (water-soluble tetrazolium salt) cell proliferation/viability assay.** HAEC cells were seeded 3000 cells per well in a 96-well plate and allowed to adhere overnight. The EGM-2 culture media was removed and replaced with EBM-2 basal media (100 µl) alone or containing SWCNT, MWCNT or CB in concentrations of 10–150 µg/10<sup>6</sup> cells or hydrogen peroxide (used as a positive control). The cells were incubated for 3 or 24 h and the WST-1 assay, which measures the formation of 2-(4-Iodophenyl)-3-(4-nitrophenyl)-5-(2,4-disulfophenyl)-2H-tetrazolium salt, was performed per the manufacturer's instructions.

**LDH (lactate dehydrogenase) cytotoxicity assay.** HAEC cells were seeded 20,000 cells per well in a 24-well plate allowed to adhere overnight. The culture media was removed and replaced with EBM-2 basal media (600 µl) alone or containing SWCNT, MWCNT or CB in concentrations of 10–150 µg/10<sup>6</sup> cells or hydrogen peroxide (used as a positive control) and the cells were cultured for 3 or 24 h. The culture media were collected at the end of the exposure, passed through a 0.2 µm syringe filters, and used in the LDH assay as instructed by the manufacturer.

**IL-8 detection assay.** Culture supernatants were collected as described above for the LDH assay. The IL-8 assay was performed as outlined by the manufacturer.

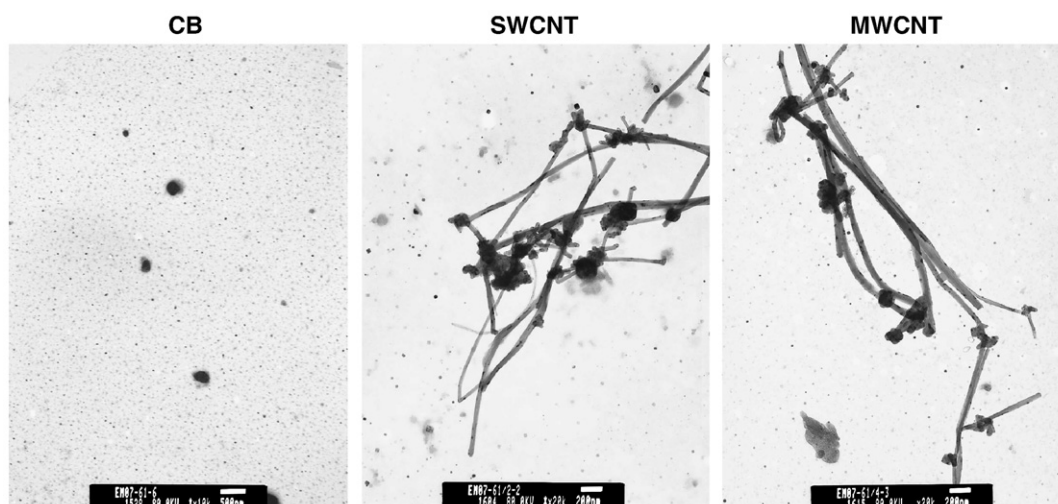


**Fig. 1.** Representative transmission electron microscopy images of carbon black (CB), single-walled carbon nanotube (SWCNT), and multi-walled carbon nanotube (MWCNT) suspensions at 1 mg/ml concentration. Scale bars: 500 nm (CB) and 200 nm (SWCNT and MWCNT).

*Actin stress filament labeling and VE-cadherin immunostaining.*

HAEC were seeded approximately 80,000 cells per well into a 4-well chamber slide and cultured overnight. The cells were exposed to particles in concentrations of 1–150  $\mu\text{g}/10^6$  cells for 3, 24, or 48 h. Cells were also treated with 100 nM PMA for 30 min as a positive control. Following incubation, cells were washed, fixed, stained, and mounted as previously described (Qian et al., 1998; Gatesman et al., 2004). VE-cadherin primary antibody was diluted 1:400 in 5% Bovine Serum Albumin (BSA) and visualized using a secondary Alexa Fluor 488 goat

anti-rabbit IgG diluted 1:200 in 5% BSA. For actin labeling, a 1:500 dilution of TRITC-phalloidin was prepared in 5% BSA. Cells were washed and mounted on slides with Fluoromount-G (Fisher). A Zeiss LSM 510 confocal microscope was used to scan images of about 1  $\mu\text{m}$  in thickness. For all figures representative images are shown (>100 cells examined per treatment).

*Tubule formation (angiogenesis assay).* HAEC were seeded at a density of 20,000 cells per well into the provided matrigel coated 96-

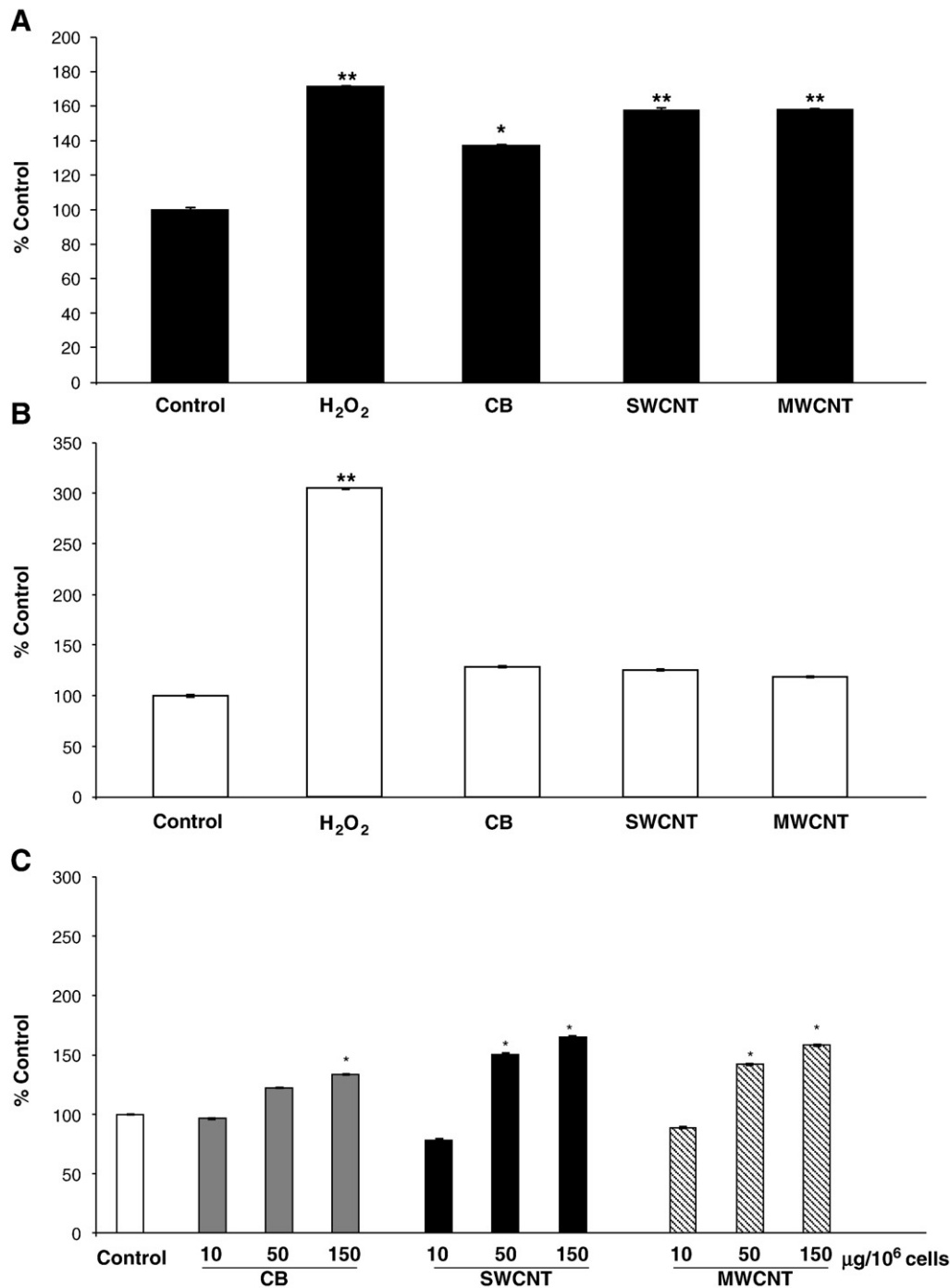


**Fig. 2.** LDH released by human aortic endothelial cells (HAEC) in a time and dose-dependent manner. An asterisk (\*) denotes a statistically significance ( $p < 0.05$  and  $**p < 0.001$ ). H<sub>2</sub>O<sub>2</sub> (500  $\mu\text{M}$ ) is used as a positive control. Values represent % of untreated control and the mean  $\pm$  SEM of three separate experiments. (A) HAEC cells exposed to 150  $\mu\text{g}/10^6$  cells (4.5  $\mu\text{g}/\text{ml}$ ) carbon black (CB), single-walled carbon nanotubes (SWCNT), or multi-walled carbon nanotubes (MWCNT) for 24 h. (B) HAEC exposed to 150  $\mu\text{g}/10^6$  cells (4.5  $\mu\text{g}/\text{ml}$ ) CB, SWCNT, or MWCNT for 3 h. (C) HAEC exposed to various concentrations (10–150  $\mu\text{g}/10^6$  cells) of CB, SWCNT, or MWCNT for 24 h.

well plate and the assay was performed per manufacturer's instructions with some modification. Briefly, HAEC cells were allowed to adhere for 1 h then the culture media was gently removed and replaced with serum-free/growth factor-free EBM-2 or EBM-2 plus 1% FBS containing SWCNT, MWCNT or CB in concentrations of 10–150  $\mu\text{g}/10^6$  cells. The plate was incubated overnight at 37 °C and 5%  $\text{CO}_2$ . Each well was examined and photographed at 10 $\times$  using the Axiovert 100 (Zeiss) microscope. Tubule formation was evaluated by measuring the tubule length as previously described (Vailhe et al., 1998).

**Transmission electron microscopy (TEM).** Particle suspensions were prepared as described above (1 mg/ml) then were further diluted in double-distilled water, loaded onto a formvar-coated copper grid, and dried. Samples were imaged using a JEOL-1220 transmission electron microscope. Cell TEM preparation, following treatment the cells were trypsinized and pelleted by centrifugation. The supernatant was gently removed and the cell pellets were fixed in Karnovsky's fixative (2.5% glutaraldehyde, 2.5% paraformaldehyde in 0.1 M Sodium Cacodylic buffer), post-fixed in osmium tetroxide, mordanted in 1% tannic acid, and stained en bloc in 0.5% uranyl acetate. The pellets were embedded in epon, sectioned, and stained with Reynold's lead citrate and uranyl acetate. Transversal sections were imaged by a JEOL 1220 transmission electron microscope.

**Statistics.** All experiments were performed a minimum of three times and all treatments were done in triplicate. Statistical significance ( $p \leq 0.05$ ) was determined using a one-way analysis of variance (ANOVA). The comparison between the treatment groups were conducted as generalized randomized complete block designs using a one-way mixed model analysis of variance with block as a random factor.

## Results

### Cytotoxicity studies

In accordance with the recent findings on the specificity of cytotoxicity assays for CNT (Worle-Knirsch et al., 2006; Casey et al., 2008), the effects of CNT on HAEC viability was evaluated under serum-free culture conditions using both LDH and WST-1 assays. First, HAEC were exposed to SWCNT, MWCNT, or CB at a concentration of 150  $\mu\text{g}/10^6$  cells (4.5  $\mu\text{g}/\text{ml}$ ) for 3 or 24 h. The exposure of HAEC cells to either SWCNT or MWCNT resulted in elevated LDH cell

release, a sign of membrane leakage, at 24 h (Fig. 2A), but not at 3 h (Fig. 2B) post-exposure. Although not in the same extent as with the CNT exposure, CB treatment also resulted in LDH release at 24 h post-exposure which is consistent with previous findings (Yamawaki and Iwai, 2006). The positive control ( $\text{H}_2\text{O}_2$ ) induced a significant release of LDH at 3 and 24 h following exposure. Second, to determine whether LDH release was dose-dependent, HAEC cells were exposed to SWCNT, MWCNT, or CB at a concentration range of 10–150  $\mu\text{g}/10^6$  cells (0.3–4.5  $\mu\text{g}/\text{ml}$ ) for 24 h. Exposure to 50 or 150  $\mu\text{g}/10^6$  cells SWCNT or MWCNT induced a significant LDH release: 151% and 165% or 142% and 158%, respectively, as compared to untreated controls (Fig. 2C). In contrast, the LDH release was not significantly increased by exposure to 50  $\mu\text{g}/10^6$  cells of CB. The 10  $\mu\text{g}/10^6$  cells concentration of either SWCNT or MWCNT did not induce LDH release by HAEC as compared to untreated controls. Furthermore, the cytotoxicity effect of CNT on HAEC was confirmed by WST-1 assay. Only the higher tested concentrations (50 and 150  $\mu\text{g}/10^6$  cells) of SWCNT (66 and 69%) and MWCNT (72 and 59%) resulted in a significant reduction in cell viability while CB had no effect (Fig. 3). The one-way mixed model analysis of variance of the WST-1 data demonstrated no difference between the effects of SWCNT and MWCNT while the response to both CNT treatments is significantly different from the one of CB treatment. Although, there is a marked difference between the surface area of SWCNT and MWCNT, they induced similar cytotoxicity which is consistent with previous reports (Koyama et al., 2006). In contrast, the surface areas of CB and MWCNT are alike but their responses are different. The data indicates that the direct contact of HAEC with either SWCNT or MWCNT results in a dose-dependent cytotoxicity.

### IL-8 ELISA

IL-8 is a main inflammatory mediator, related to chemical-mediated cytotoxic responses (Simeonova and Luster, 1996). Exposure of HAEC cells to 50 or 150  $\mu\text{g}/10^6$  cells to either SWCNT or MWCNT resulted in a minimal but significant increase in IL-8 released at 24 h post-exposure as compared to controls (Fig. 4). HAEC exposed to CB did not induce the release of IL-8. Further, low concentrations (1–10  $\mu\text{g}/10^6$  cells) of SWCNT or MWCNT for 24 h as well as exposure to 50–150  $\mu\text{g}/10^6$  cells for 3 h did not induce a significant release of IL-8 (data not shown). Thus, IL-8 results were consistent with the cytotoxicity findings including LDH release and WST-1 viability.

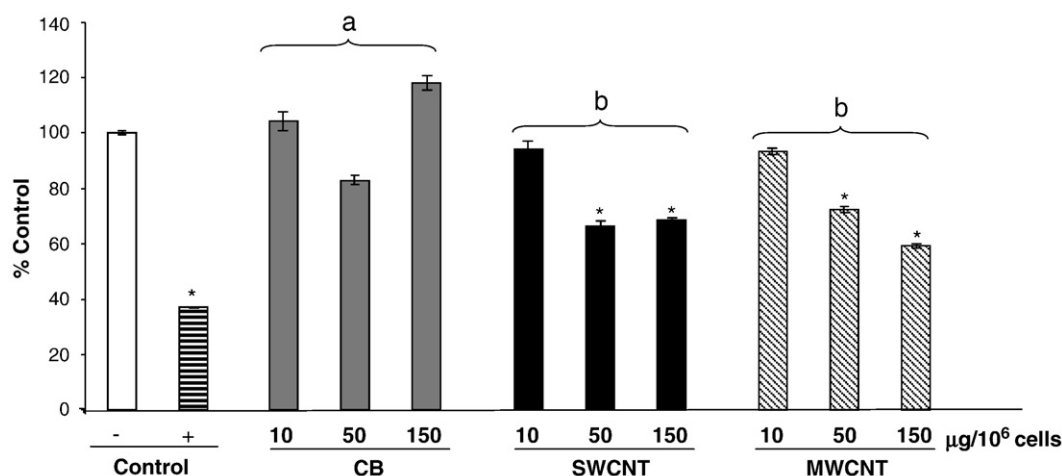


**Fig. 3.** Cell viability of human aortic endothelial cells (HAEC) measured by WST-1 assay. HAEC were exposed to carbon black (CB), single-walled carbon nanotubes (SWCNT) or multi-walled carbon nanotubes (MWCNT) in concentrations of 10–150  $\mu\text{g}/10^6$  cells (0.3–4.5  $\mu\text{g}/\text{ml}$ ) for 24 h.  $\text{H}_2\text{O}_2$  (500  $\mu\text{M}$ ) was used as a positive control. Values represent % of untreated control and the mean  $\pm$  SEM of three separate experiments. An asterisk (\*) denotes a statistically significant difference from the negative control; different letters (a, b) denote a statistically significant difference between treatment groups ( $p < 0.05$ ).



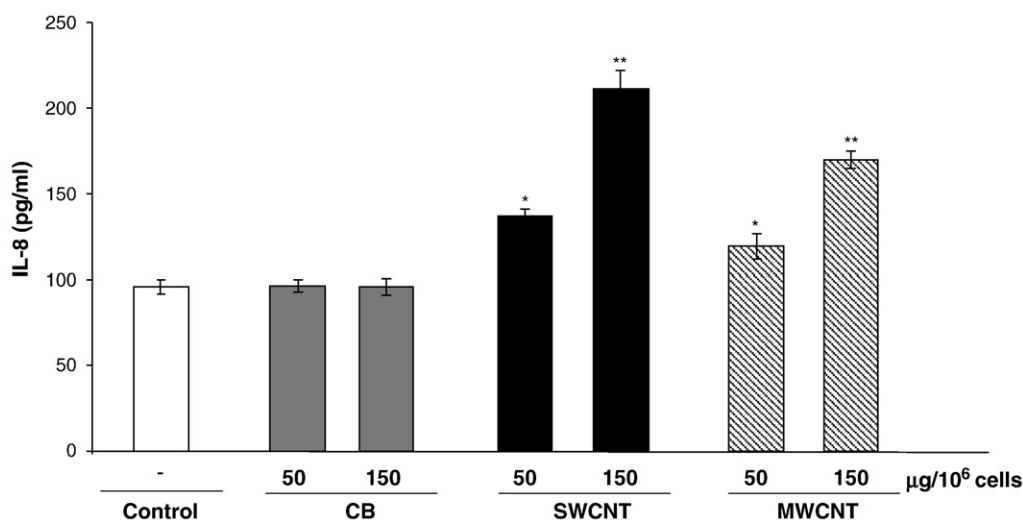


**Fig. 4.** IL-8 released by human aortic endothelial cells (HAEC). HAEC were exposed to carbon black (CB), single-walled carbon nanotubes (SWCNT) or multi-walled carbon nanotubes (MWCNT) in concentrations of 50 or 150 µg/10<sup>6</sup> cells (1.5–4.5 µg/ml) for 24 h. An asterisk (\*) denotes a statistically significance (\**p*<0.05 and \*\**p*<0.001). Values represent % of untreated control and the mean ± SEM of three separate experiments.

#### Actin and VE-cadherin visualization

The cytoskeleton plays a major role in the physiology of endothelial cells including adhesion, permeability, vasculogenesis, and motility (Moreau et al., 2003). The actin filaments were stained with TRITC-phalloidin (Fig. 5A). HAEC cultured in control conditions displayed both cortical (peripheral) and stress fibers. A similar actin organization was observed in cells treated with CB at all tested concentrations. In contrast, brief treatment (30 min) with PMA, used as a positive control, caused a marked disruption of the actin cytoskeleton. Exposure of HAEC to high concentrations (50 and 150 µg/10<sup>6</sup> cells) of SWCNT or MWCNT also resulted in a marked disruption in actin filaments by 24 h (representative images of HAEC treated with 50 µg/10<sup>6</sup> cells are shown in Fig. 5A). However, exposure to SWCNT, MWCNT, or CB at lower concentrations (1–10 µg/10<sup>6</sup> cells) for 24 h (Supplemental data Fig. S1) as well as to any of the tested concentrations for 3 h did not demonstrate changes in actin filament integrity (data not shown). Furthermore, longer exposure (48 h) in low concentrations (1–10 µg/10<sup>6</sup> cells) did not induce actin disruption but the highest concentration (150 µg/10<sup>6</sup> cells) did show changes (Supplemental data Fig. S2). To determine whether the CNT-induced actin filament disruption is a result of direct association of the particles with the cells, the visualization of the particles and actin filaments was analyzed using both differential interference contrast (DIC) and fluorescence microscopy (Fig. 5B). Actin filament rearrangement was correlated to direct contact of SWCNT or MWCNT with the HAEC cells. Interestingly, CB, although not associated with actin cytoskeleton alterations, appeared to be localized in the perinuclear region of the cell as reported previously (Yamawaki and Iwai, 2006).

VE-cadherin is the main component of the adherens junctions (AJ) comprising the endothelial barrier (reviewed in Vandenbroucke et al., 2008). Dynamic interactions between the AJ proteins and actin cytoskeleton are crucial in regulation of endothelium intercellular contacts and permeability. VE-cadherin localization was characterized by immunostaining (Fig. 6). Positive VE-cadherin was observed along the contours of the cell membrane of untreated or CB treated HAEC. The peripheral VE-cadherin staining was markedly reduced in the majority of the HAEC treated with 50 or 150 µg/10<sup>6</sup> cells of either MWCNT or SWCNT for 24 h (representative images of cells treated with 150 µg/10<sup>6</sup> cells shown in Fig. 6). Simultaneous VE-cadherin and actin staining demonstrated CNT-induced co-localized actin and VE-cadherin disruption (Fig. 6). However, consistent with the actin findings, 24 h exposure to lower concentrations (1–10 µg/10<sup>6</sup> cells) of

SWCNT or MWCNT did not affect the VE-cadherin staining (data not shown). Further, regular VE-cadherin staining was observed at 3 h post-exposure in all tested concentrations (data not shown).

#### TEM

In an attempt to explore in more detail the cell localization of CNT, TEM imaging was conducted (Fig. 7). A small number of CNT were identified in the cytoplasm of some cells as well as between cells along the cell membrane which may result in alterations in cell–cell contact interactions consistent with the VE-cadherin findings (representative images of HAEC treated with SWCNT 150 µg/10<sup>6</sup> cells are shown). The general morphology of HAEC cells, which was associated with the CNT, was similar to that of untreated cells.

#### Tubule formation

Tubule formation (angiogenesis) is one of the main functions of intact endothelial cells (Horowitz and Simons, 2008). To determine whether CNT exposure affects overall endothelial cell behavior, we evaluated CNT effect on tubule formation (Figs. 8 A and B). HAEC cells formed a well organized tubule network (Fig. 8A). However, exposure to 50–150 µg/10<sup>6</sup> cells to either SWCNT or MWCNT resulted in a marked disruption of the tubule network. The effect was observed under culture conditions including media free of growth factors and serum as well as media containing 1% FBS (the latter known to support endothelial cell tubule formation). The treatment of these cells with PMA resulted in an increase in network complexity and tubule length (data not shown). The lower tested CNT concentrations (10 µg/10<sup>6</sup> cells) did not induce significant destruction of tubule formation (data not shown). Quantification of tubule length confirmed the microscopic observations on the effect of CNT exposure on tubule formation (Fig. 8B).

#### Discussion

The functionality of endothelial cells is fundamental for the homeostasis of the vascular system (Cai and Harrison, 2000). Due to its unique position in the vessel wall, the endothelium acts as a barrier and serves as the primary sensor for normal blood flow. The findings of this study demonstrated actin cytoskeleton disruption accompanied with altered VE-cadherin localization, reduced tubule formation, and a concomitant diminished viability of human aortic endothelial cells as a result of exposure to purified SWCNT or MWCNT. These

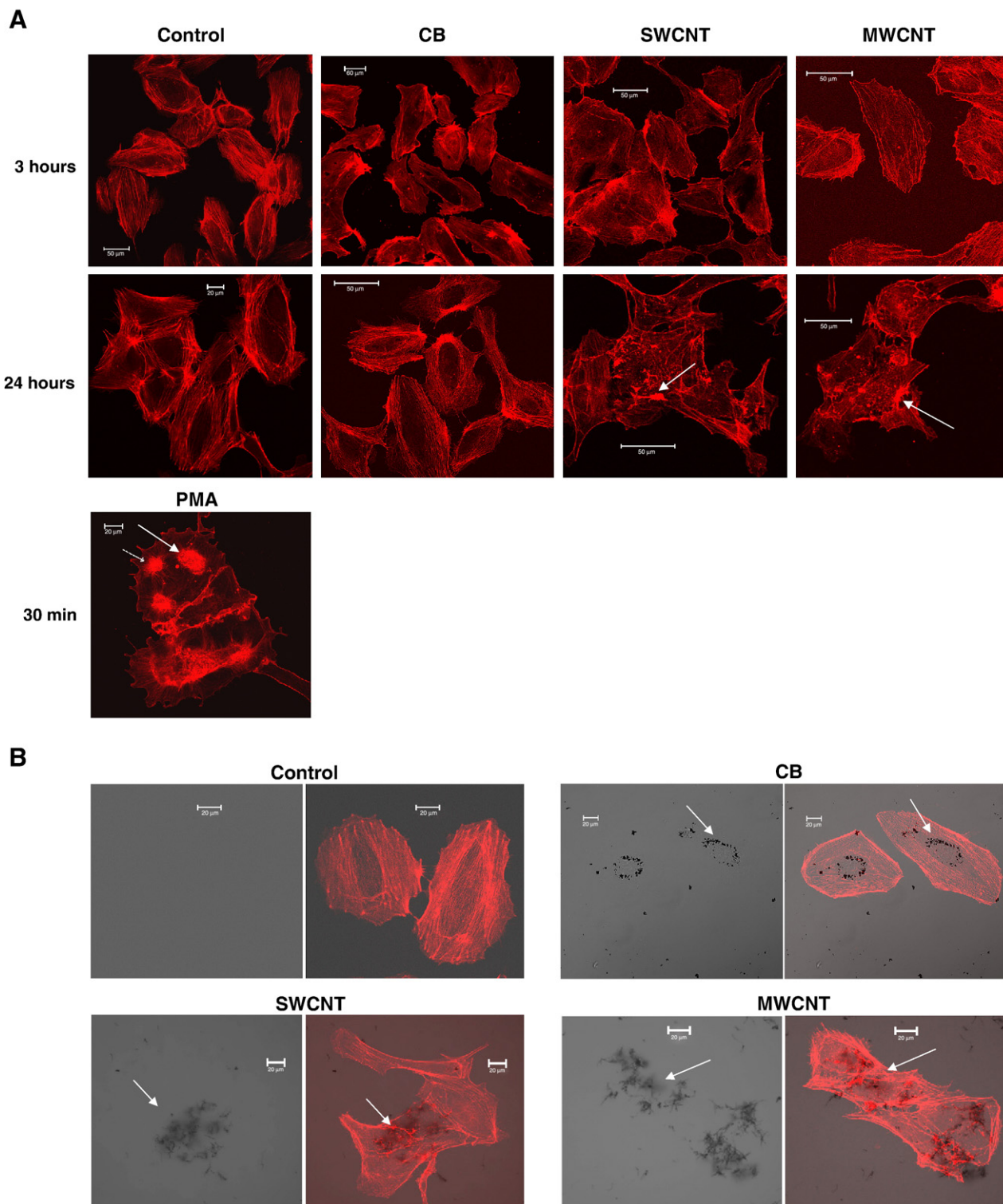


**Fig. 5.** Representative confocal microscope images of actin cytoskeleton organization in human aortic endothelial cells (HAEC) and visualization of particle–cell interactions. (A) Actin staining with TRITC-phalloidin. HAEC were exposed to carbon black (CB), single-walled carbon nanotubes (SWCNT) or multi-walled carbon nanotubes (MWCNT) in concentrations of  $50 \mu\text{g}/10^6$  cells ( $1.5 \mu\text{g}/\text{ml}$ ). PMA ( $100 \text{ nM}$ ) was used as a positive control. Scale bar:  $50 \mu\text{m}$ . The arrows indicate actin disruption. (B) Actin cytoskeleton visualized by fluorescence of TRITC-phalloidin and particles by differential interference contrast (DIC) microscopy. HAEC were exposed to  $150 \mu\text{g}/10^6$  cells ( $4.5 \mu\text{g}/\text{ml}$ ) CB, SWCNT, or MWCNT for 24 h. Scale bar:  $20 \mu\text{m}$ . The arrows indicate co-localization of CNT and disruption actin.

effects were dose-dependent and most likely associated with mechanical damage to the cell membrane. The endothelial cells tolerated the low concentrations of carbon nanotubes without changes in viability, cytoskeleton, and function. The findings can help to explain potential lung and cardiovascular effects related to CNT

respiratory exposure. CNT inhaled in the lung will be in concentrations sufficient to induce direct toxicity to many cells including the endothelial which will facilitate leakage of inflammatory mediators into the systemic circulation. Recently, we demonstrated that an acute respiratory exposure to CNT resulted in lung inflammatory and stress



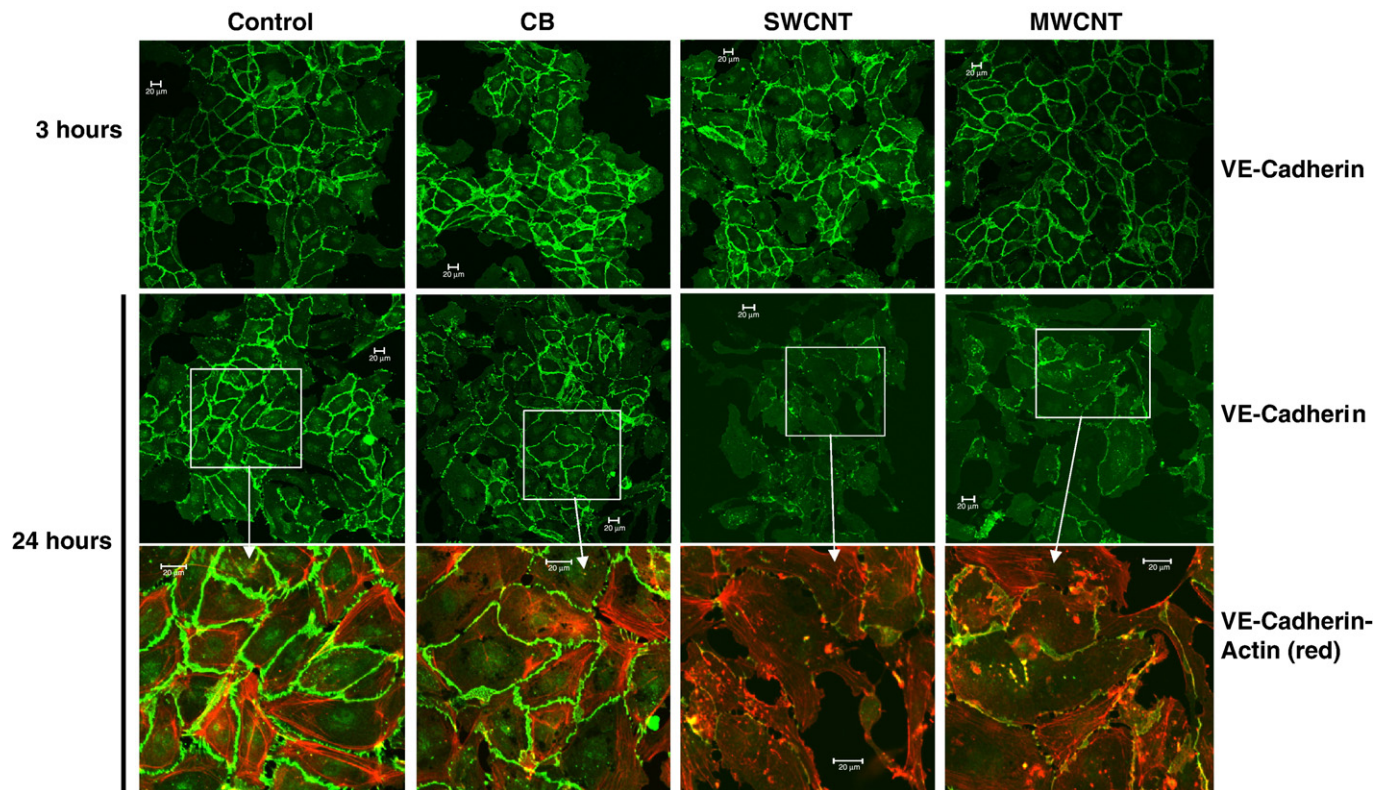


**Fig. 6.** Representative confocal microscope images of VE-cadherin immunostaining of human aortic endothelial cells (HAEC). HAEC were exposed to  $150 \mu\text{g}/10^6$  cells ( $4.5 \mu\text{g}/\text{ml}$ ) carbon black (CB), single-walled carbon nanotubes (SWCNT) or multi-walled carbon nanotubes (MWCNT). The squared areas are shown below as merged of VE-cadherin (green) and actin filament (red) staining. Scale bar:  $20 \mu\text{m}$ .

responses with a concomitant release of soluble biomarkers of inflammation and coagulation into the systemic circulation (Erdelyi et al., 2009). Translocation of CNT from the lung into the systemic bloodstream remains debated. Based on animal studies conducted with several types of nanoparticles, systemic blood translocation may occur but probably in low concentrations which may not induce direct cytotoxicity (Kreyling et al., 2002; Nemmar et al., 2002; Oberdorster et al., 2002; Mills et al., 2008b). Hypothetically, translocation of CNT from the lung into the systemic circulation, even in low concentrations, if associated with penetration and biopersistent accumulation

into the vascular wall may induce chronic effects and potential adverse cardiovascular outcomes.

The cytoskeleton plays an essential role in many cellular processes including maintaining cellular shape, organelle transport, cell polarity, cell division, exocytosis, and formation of motility structures (Goode et al., 2000). A multitude of signaling proteins work together with actin filaments to regulate cell shape, localize signaling complexes to specific locations within the cell, and generate the protrusive force needed for membrane projections and cell motility (Goode et al., 2000; Carlier et al., 2003). Furthermore, the interaction between the

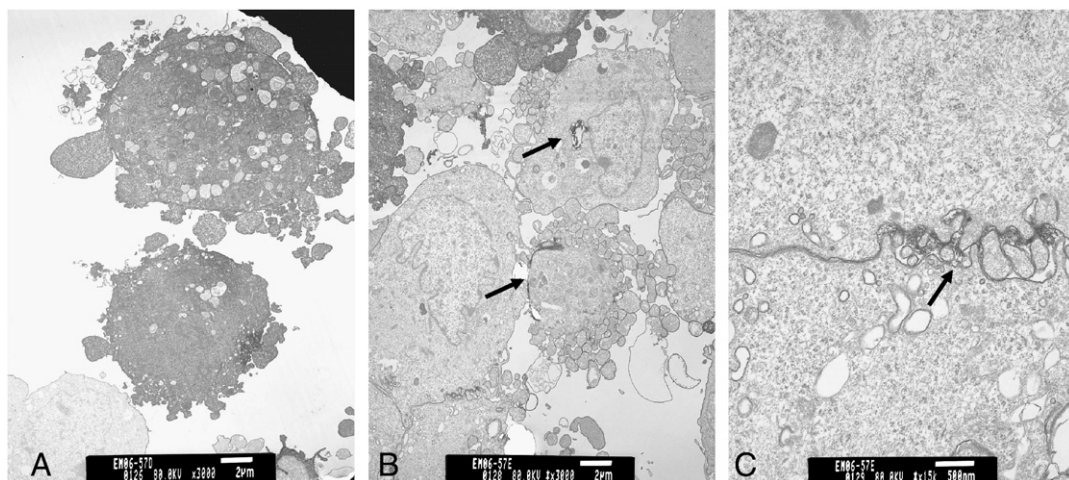


**Fig. 7.** Representative transmission electron microscopy images of human aortic endothelial cells (HAEC). HAEC in culture basal media without growth factors (EBM) and were left untreated (A) or exposed to  $150 \mu\text{g}/10^6$  cells ( $4.5 \mu\text{g}/\text{ml}$ ) single-walled carbon nanotubes (SWCNT) for 24 h exposure (B and C). The arrows indicate SWCNT localization. Scale bar:  $2 \mu\text{m}$ . Panel C is a higher magnification of (B) to show SWCNT between cells. Scale bar:  $500 \text{ nm}$ .

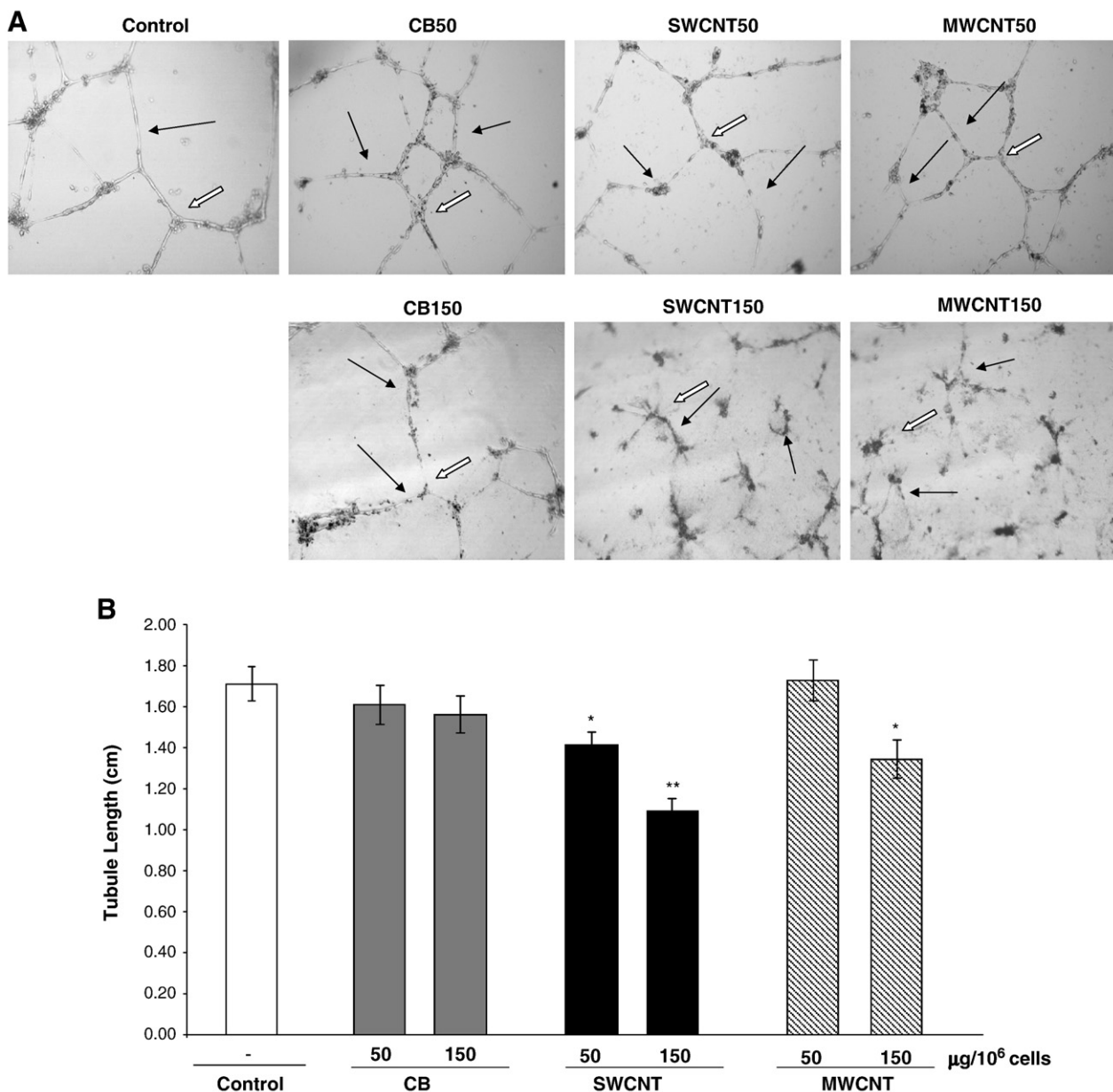


**Fig. 8.** Tubule formation of human aortic endothelial cells (HAEC). (A) Representative images of HAEC tubule formation. HAEC were exposed to carbon black (CB), single-walled carbon nanotubes (SWCNT) or multi-walled carbon nanotubes (MWCNT) in concentrations of 50–150  $\mu\text{g}/10^6 \text{ cells}$  (1.5–4.5  $\mu\text{g}/\text{ml}$ ) for 24 h. Solid arrows indicate tubules and open arrows indicate branch points. (B) Quantification of the CNT-induced changes in HAEC tubule formation. Tubule length was measured of all images generated and presented as mean length (cm)  $\pm$  SEM. An asterisk (\*) denotes a statistically significance (\* $p < 0.05$  and \*\* $p < 0.001$ ).

actin cytoskeleton and VE-cadherin complex plays an important role in maintaining normal endothelial barrier permeability and function (Bootle-Wilbraham et al., 2000; Kovacs et al., 2002). The linkage of the actin cytoskeleton to cell–cell junctions has been well studied. Filamentous actin is physically tethered to these junctions and any significant changes associated with the actin cytoskeleton would in theory promote an alteration in the cell–cell junctions (Hartsock and Nelson, 2008; Miyoshi and Takai, 2008). Here we demonstrated that direct contact between CNT and endothelial cells resulted in disruption of the actin cytoskeleton and the intercellular interactions which may have multiple effects on endothelium function. In contrast, CB particles, which are completely internalized into the cells, did not induce significant modification of the endothelial cell integrity or function. Well characterized disruptors of endothelial cell cytoskeleton and cell–cell contacts, such as thrombin and TNF- $\alpha$ , induce fast, in the first 3 h after exposure, microfilament rearrangement and

compromised VE-cadherin intercellular contacts (Vouret-Craviari et al., 1998; Petrache et al., 2003). These effects are associated with specific ligand–receptor interactions and triggering of related signaling pathways (Vandenbroucke et al., 2008). The CNT-induced effects including impaired cell function and viability, which did not occur in the first 3 h after exposure, are most likely associated with mechanical damage to the cell membrane. Marked actin disorganization was correlated with regions of higher CNT density. Consistent with our findings, recent studies exploring the cytotoxicity of MWCNT on mouse macrophage cell line suggested that the cell injury is a result of membrane rupturing or shearing but did not involve activation of MAP kinases and other specific death pathways (Hirano et al., 2008). Direct and more detailed imaging of SWCNT, using modified methods of TEM and confocal microscopy in human monocyte-derived macrophages, has identified intracellular bundles which fused and aligned with their long axes parallel to the plasma membrane (Porter et al., 2007).



Moreover, these studies have demonstrated lysosomal and nuclear localization of SWCNT after several days of exposure (4 days). These authors suggested active uptake by phagocytosis and passive uptake through the lipid membrane bilayer. The latter may have an implication in the interaction of CNT with endothelial cells. Furthermore, it has been demonstrated that MWCNT-induced cytotoxicity of keratinocytes involves engulfment and intracellular localization of the particles (Monteiro-Riviere et al., 2005). The mechanisms leading to direct effects of CNT on target cells vary depending on the cell type, state of particle aggregation, purity, concentration, and other experimental parameters.

Overall, the findings of our current studies demonstrated that CNT direct contact with endothelial cells triggers a dose-dependent impaired cell function and viability accompanied with the actin cytoskeleton and intercellular contact disruption.

#### Conflict of interest statement

The authors of this manuscript declare there are no conflicts of interest.

#### Disclaimer

The findings and conclusions in this report are those of the authors and do not necessarily represent the views of the National Institute for Occupational Safety and Health.

#### Appendix A. Supplementary data

Supplementary data associated with this article can be found, in the online version, at doi:10.1016/j.taap.2009.02.018.

#### References

- Bootle-Wilbraham, C.A., Tazzyman, S., Marshall, J.M., Lewis, C.E., 2000. Fibrinogen E-fragment inhibits the migration and tubule formation of human dermal microvascular endothelial cells in vitro. *Cancer Res.* 60, 4719–4724.
- Borm, P.J., Robbins, D., Haubold, S., Kuhlbusch, T., Fissan, H., Donaldson, K., Schins, R., Stone, V., Kreyling, W., Lademann, J., Krutmann, J., Warheit, D., Oberdorster, E., 2006. The potential risks of nanomaterials: a review carried out for ECETOC. *Part Fibre Toxicol.* 3, 11.
- Brook, R.D., Franklin, B., Cascio, W., Hong, Y., Howard, G., Lipsett, M., Luepker, R., Mittleman, M., Samet, J., Smith Jr., S.C., Tager, I., 2004. Air pollution and cardiovascular disease: a statement for healthcare professionals from the Expert Panel on Population and Prevention Science of the American Heart Association. *Circulation* 109, 2655–2671.
- Cai, H., Harrison, D.G., 2000. Endothelial dysfunction in cardiovascular diseases: the role of oxidant stress. *Circ. Res.* 87, 840–844.
- Carlier, M.F., Le Clainche, C., Wiesner, S., Pantaloni, D., 2003. Actin-based motility: from molecules to movement. *Bioessays* 25, 336–345.
- Casey, A., Herzog, E., Lyng, F.M., Byrne, H.J., Chambers, G., Davoren, M., 2008. Single walled carbon nanotubes induce indirect cytotoxicity by medium depletion in A549 lung cells. *Toxicol. Lett.* 179, 78–84.
- Donaldson, K., Aitken, R., Tran, L., Stone, V., Duffin, R., Forrest, G., Alexander, A., 2006. Carbon nanotubes: a review of their properties in relation to pulmonary toxicology and workplace safety. *Toxicol. Sci.* 92, 5–22.
- Erdely, A., Hulderman, T., Salmen, R., Liston, A., Zeidler-Erdely, P.C., Schwegler-Berry, D., Castranova, V., Koyama, S., Kim, Y.A., Endo, M., Simeonova, P.P., 2009. Cross-talk between lung and systemic circulation during carbon nanotube respiratory exposure. *Potential Biomarkers Nano Lett.* 9, 36–43.
- Gatesman, A., Walker, V.G., Baisden, J.M., Weed, S.A., Flynn, D.C., 2004. Protein kinase C $\alpha$  activates c-Src and induces podosome formation via AFAP-110. *Mol. Cell Biol.* 24, 7578–7597.
- Goode, B.L., Drubin, D.G., Barnes, G., 2000. Functional cooperation between the microtubule and actin cytoskeletons. *Curr. Opin. Cell Biol.* 12, 63–71.
- Hartsock, A., Nelson, W.J., 2008. Adherens and tight junctions: structure, function and connections to the actin cytoskeleton. *Biochim. Biophys. Acta* 1778, 660–669.
- Heckel, K., Kieffmann, R., Dorger, M., Stoeckelhuber, M., Goetz, A.E., 2004. Colloidal gold particles as a new in vivo marker of early acute lung injury. *Am. J. Physiol., Lung Cell Mol. Physiol.* 287, L867–L878.
- Hirano, S., Kanno, S., Furuyama, A., 2008. Multi-walled carbon nanotubes injure the plasma membrane of macrophages. *Toxicol. Appl. Pharmacol.* 232, 244–251.
- Horowitz, A., Simons, M., 2008. Branching morphogenesis. *Circ. Res.* 103, 784–795.
- Kim, Y.A., Hayashi, T., Endo, M., Kaburagi, Y., Tsukada, T., Shan, J., Osato, K., Tsuruoka, S., 2005. Synthesis and structural characterization of thin multi-walled carbon nanotubes with a partially faceted cross section by a floating reactant method. *Carbon* 43, 2243–2250.
- Kovacs, E.M., Goodwin, M., Ali, R.G., Paterson, A.D., Yap, A.S., 2002. Cadherin-directed actin assembly: E-cadherin physically associates with the Arp2/3 complex to direct actin assembly in nascent adhesive contacts. *Curr. Biol.* 12, 379–382.
- Koyama, S., Endo, M., Kim, Y.-A., Hayashi, T., Yanagisawa, T., Osaka, K., Koyama, H., Haniu, H., Kuroiwa, N., 2006. Role of systemic T-cells and histopathological aspects after subcutaneous implantation of various carbon nanotubes in mice. *Carbon* 44, 1079–1092.
- Kreyling, W.G., Semmler, M., Erbe, F., Mayer, P., Takenaka, S., Schulz, H., Oberdorster, G., Ziesenis, A., 2002. Translocation of ultrafine insoluble iridium particles from lung epithelium to extrapulmonary organs is size dependent but very low. *J. Toxicol. Environ. Health* 65, 1513–1530.
- Lam, C.W., James, J.T., McCluskey, R., Hunter, R.L., 2004. Pulmonary toxicity of single-wall carbon nanotubes in mice 7 and 90 days after intratracheal instillation. *Toxicol. Sci.* 77, 126–134.
- Li, J.G., Li, W.X., Xu, J.Y., Cai, X.Q., Liu, R.L., Li, Y.J., Zhao, Q.F., Li, Q.N., 2007a. Comparative study of pathological lesions induced by multiwalled carbon nanotubes in lungs of mice by intratracheal instillation and inhalation. *Environ. Toxicol.* 22, 415–421.
- Li, Z., Hulderman, T., Salmen, R., Chapman, R., Leonard, S.S., Young, S.H., Shvedova, A., Luster, M.I., Simeonova, P.P., 2007b. Cardiovascular effects of pulmonary exposure to single-wall carbon nanotubes. *Environ. Health Perspect.* 115, 377–382.
- Mangum, J.B., Turpin, E.A., Antao-Menezes, A., Cesta, M.F., Bermudez, E., Bonner, J.C., 2006. Single-walled carbon nanotube (SWCNT)-induced interstitial fibrosis in the lungs of rats is associated with increased levels of PDGF mRNA and the formation of unique intercellular carbon structures that bridge alveolar macrophages in situ. *Part Fibre Toxicol.* 3, 15.
- Manna, S.K., Sarkar, S., Barr, J., Wise, K., Barrera, E.V., Jejelowo, O., Rice-Ficht, A.C., Ramesh, G.T., 2005. Single-walled carbon nanotube induces oxidative stress and activates nuclear transcription factor-kappaB in human keratinocytes. *Nano Lett.* 5, 1676–1684.
- Maynard, A.D., Aitken, R.J., Butz, T., Colvin, V., Donaldson, K., Oberdorster, G., Philbert, M.A., Ryan, J., Seaton, A., Stone, V., Tinkle, S.S., Tran, L., Walker, N.J., Warheit, D.B., 2006. Safe handling of nanotechnology. *Nature* 444, 267–269.
- Mercer, R.R., Scabilloni, J., Wang, L., Kisin, E., Murray, A.R., Schwegler-Berry, D., Shvedova, A.A., Castranova, V., 2008. Alteration of deposition pattern and pulmonary response as a result of improved dispersion of aspirated single-walled carbon nanotubes in a mouse model. *Am. J. Physiol., Lung Cell Mol. Physiol.* 294, L87–L97.
- Mills, N.L., Tornqvist, H., Robinson, S.D., Gonzalez, M.C., Soderberg, S., Sandstrom, T., Blomberg, A., Newby, D.E., Donaldson, K., 2007. Air pollution and atherothrombosis. *Inhal. Toxicol.* 19 (Suppl. 1), 81–89.
- Mills, N.L., Miller, J.J., Anand, A., Robinson, S.D., Frazer, G.A., Anderson, D., Breen, L., Wilkinson, I.B., McEniery, C.M., Donaldson, K., Newby, D.E., Macnee, W., 2008a. Increased arterial stiffness in patients with chronic obstructive pulmonary disease: a mechanism for increased cardiovascular risk. *Thorax* 63, 306–311.
- Mills, N.L., Oberdorster, G., Newby, D.E., 2008b. Reducing exposure to airborne particles: a novel strategy to improve cardiovascular health. *Am. J. Respir. Crit. Care Med.* 177, 366–367.
- Miyoshi, J., Takai, Y., 2008. Structural and functional associations of apical junctions with cytoskeleton. *Biochim. Biophys. Acta* 1778, 670–691.
- Monteiro-Riviere, N.A., Nemanich, R.J., Inman, A.O., Wang, Y.Y., Riviere, J.E., 2005. Multi-walled carbon nanotube interactions with human epidermal keratinocytes. *Toxicol. Lett.* 155, 377–384.
- Moreau, V., Tatin, F., Varon, C., Genot, E., 2003. Actin can reorganize into podosomes in aortic endothelial cells, a process controlled by Cdc42 and RhoA. *Mol. Cell Biol.* 23, 6809–6822.
- Muller, J., Huau, F., Moreau, N., Misson, P., Heilier, J.F., Delos, M., Arras, M., Fonseca, A., Nagy, J.B., Lison, D., 2005. Respiratory toxicity of multi-wall carbon nanotubes. *Toxicol. Appl. Pharmacol.* 207, 221–231.
- Nemmar, A., Hoet, P.H., Vanquickenborne, B., Dinsdale, D., Thomeer, M., Hoylaerts, M.F., Vanbilloen, H., Mortelmans, L., Nemery, B., 2002. Passage of inhaled particles into the blood circulation in humans. *Circulation* 105, 411–414.
- Oberdorster, G., Sharp, Z., Atudorei, V., Elder, A., Gelein, R., Lunts, A., Kreyling, W., Cox, C., 2002. Extrapulmonary translocation of ultrafine carbon particles following whole-body inhalation exposure of rats. *J. Toxicol. Environ. Health* 65, 1531–1543.
- Oberlin, A., Endo, M., Koyama, T., 1976. Filamentous growth of carbon through benzene decomposition. *J. Cryst. Growth* 32, 335–349.
- Pacurari, M., Yin, X.J., Ding, M., Leonard, S.S., Schwegler-Berry, D., Ducatman, B.S., Chirila, M., Endo, M., Castranova, V., Vallyathan, V., 2008a. Oxidative and molecular interactions of multi-wall carbon nanotubes (MWCNT) in normal and malignant human mesothelial cells. *Nanotoxicology* 2, 155–170.
- Pacurari, M., Yin, X.J., Zhao, J., Ding, M., Leonard, S.S., Schwegler-Berry, D., Ducatman, B.S., Sbarra, D., Hoover, M.D., Castranova, V., Vallyathan, V., 2008b. Raw single-wall carbon nanotubes induce oxidative stress and activate MAPKs, AP-1, NF-kappaB, and Akt in normal and malignant human mesothelial cells. *Environ. Health Perspect.* 116, 1211–1217.
- Petrache, I., Birukova, A., Ramirez, S.I., Garcia, J.G., Verin, A.D., 2003. The role of the microtubules in tumor necrosis factor-alpha-induced endothelial cell permeability. *Am. J. Respir. Cell Mol. Biol.* 28, 574–581.
- Porter, A.E., Gass, M., Muller, K., Skepper, J.N., Midgley, P.A., Welland, M., 2007. Direct imaging of single-walled carbon nanotubes in cells. *Nat. Nanotechnology* 2, 713–717.
- Qian, Y., Baisden, J.M., Westin, E.H., Guappone, A.C., Koay, T.C., Flynn, D.C., 1998. Src can regulate carboxy terminal interactions with AFAP-110, which influence self-association, cell localization and actin filament integrity. *Oncogene* 16, 2185–2195.
- Raja, P.M., Connolly, J., Ganesan, G.P., Ci, L., Ajayan, P.M., Nalamasu, O., Thompson, D.M., 2007. Impact of carbon nanotube exposure, dosage and aggregation on smooth muscle cells. *Toxicol. Lett.* 169, 51–63.
- Shvedova, A.A., Castranova, V., Kisin, E.R., Schwegler-Berry, D., Murray, A.R., Gandelsman, V.Z., Maynard, A., Baron, P., 2003. Exposure to carbon nanotube material:

- assessment of nanotube cytotoxicity using human keratinocyte cells. *J. Toxicol. Environ. Health* 66, 1909–1926.
- Shvedova, A.A., Kisin, E.R., Mercer, R., Murray, A.R., Johnson, V.J., Potapovich, A.I., Tyurina, Y.Y., Gorelik, O., Arepalli, S., Schwegler-Berry, D., Hubbs, A.F., Antonini, J., Evans, D.E., Ku, B.K., Ramsey, D., Maynard, A., Kagan, V.E., Castranova, V., Baron, P., 2005. Unusual inflammatory and fibrogenic pulmonary responses to single-walled carbon nanotubes in mice. *Am. J. Physiol., Lung Cell. Mol. Physiol.* 289, L698–L708.
- Simeonova, P.P., Luster, M.I., 1996. Asbestos induction of nuclear transcription factors and interleukin 8 gene regulation. *Am. J. Respir. Cell Mol. Biol.* 15, 787–795.
- Vailhe, B., Lecomte, M., Wiernsperger, N., Tranqui, L., 1998. The formation of tubular structures by endothelial cells is under the control of fibrinolysis and mechanical factors. *Angiogenesis* 2, 331–344.
- Vandenbroucke, E., Mehta, D., Minshall, R., Malik, A.B., 2008. Regulation of endothelial junctional permeability. *Ann. N.Y. Acad. Sci.* 1123, 134–145.
- Vouret-Craviari, V., Boquet, P., Pouyssegur, J., Van Obberghen-Schilling, E., 1998. Regulation of the actin cytoskeleton by thrombin in human endothelial cells: role of Rho proteins in endothelial barrier function. *Mol. Biol. Cell* 9, 2639–2653.
- Warheit, D.B., Laurence, B.R., Reed, K.L., Roach, D.H., Reynolds, G.A., Webb, T.R., 2004. Comparative pulmonary toxicity assessment of single-wall carbon nanotubes in rats. *Toxicol. Sci.* 77, 117–125.
- Worle-Knirsch, J.M., Pulskamp, K., Krug, H.F., 2006. Oops they did it again! Carbon nanotubes hoax scientists in viability assays. *Nano Lett.* 6, 1261–1268.
- Yamawaki, H., Iwai, N., 2006. Mechanisms underlying nano-sized air-pollution-mediated progression of atherosclerosis: carbon black causes cytotoxic injury/inflammation and inhibits cell growth in vascular endothelial cells. *Circ. J.* 70, 129–140.